emerald insight

Journal of Structural Fire Engineering

Cold-formed steel columns at both ambient and fire conditions
Hélder Craveiro, João Paulo Correia Rodrigues, Luis Laim,

Article information:

For Authors

If you would like to write for this, or any other Emerald publication, then please use our Emerald for Authors service information about how to choose which publication to write for and submission guidelines are available for all. Please visit www.emeraldinsight.com/authors for more information.

About Emerald www.emeraldinsight.com

Emerald is a global publisher linking research and practice to the benefit of society. The company manages a portfolio of more than 290 journals and over 2,350 books and book series volumes, as well as providing an extensive range of online products and additional customer resources and services.

Emerald is both COUNTER 4 and TRANSFER compliant. The organization is a partner of the Committee on Publication Ethics (COPE) and also works with Portico and the LOCKSS initiative for digital archive preservation.

Cold-formed steel columns at both ambient and fire conditions

Hélder Craveiro
University of Coimbra, Coimbra, Portugal, and

João Paulo Correia Rodrigues and Luis Laim
Department of Civil Engineering, Universidade de Coimbra, Coimbra, Portugal

Abstract

Purpose – The use of cold-formed steel members has increased significantly in the past few years; however, its design is only briefly addressed in the current design codes, such as the EN 1993-1-3. To evaluate the compressive behavior of single and built-up cold-formed steel members, at ambient and simulated fire conditions with restrained thermal elongation, experimental and numerical tests were undertaken.

Design/methodology/approach – Four cross-section shapes were tested, namely, one single (lipped channel), one open built-up (I) and two closed built-up (R and 2R), considering two end support conditions, pinned and fixed. Two test set-ups were specifically developed for these tests. Based on the experimental results finite element models were developed and calibrated to allow future parametric studies.

Findings – This paper showed that increasing the level of restraint to thermal elongation and the initially applied load led to lower critical temperatures. Increasing the level of restraint to thermal elongation, the failure is governed by the generated axial restraining forces, whereas for lower levels of restraint to thermal elongation, the failure is controlled by the temperature increasing.

Originality/value – This paper is a contribution to the knowledge on the behavior of cold-formed steel columns subjected to fire, especially on the ones with a built-up cross-section, where results on thermal restrained ones are still scarce. It presented a set of experimental and numerical results useful for the development of numerical and analytical analysis concerning the development of new simplified calculation methods.

Keywords Buckling, Fire, Ambient temperature, Cold-formed steel, Column, Restraining

Paper type Research paper

Notation

A_{eff} = Effective cross-sectional area;
A_g = Gross cross-sectional area;
CFS = Cold-formed steel;
CV = Coefficient of variation;
d = Lateral deformation;
d_v = Axial displacement;
E_θ = Modulus of elasticity;
f = Stress;
f_{ya} = Average yield strength;

f_{yb}	= Basic yield strength;
$f_{y.\theta}$	= Yield strength at temperature θ (°C);
$f_{u.\theta}$	= Ultimate strength;
L	= Height of the column;
P	= Axial restraining force generated in the column;
P_O	= Initial applied load to the column;
P_{max}	= Maximum axial force generated in the column;
ε_θ	= Strain at temperature θ (°C);
$\varepsilon_{r.\theta}$	= Strain at rupture;
$\varepsilon_{us.\theta}$	= Plastic strain at maximum tension load;
$\overline{\theta}_c$	= Mean temperature of the column (°C);
θ_{cr}	= Critical temperature of the column; and
$\overline{\theta}_{s.i}$	= Mean temperature of the cross-section i.

1. Introduction

Nowadays, in the light steel framing construction industry, individual profiles with different cross-section shapes (C, U, Σ, etc.) are used to fabricate built-up members. A built-up cold-formed steel (CFS) structural member can span more distance and present higher load bearing capacity and torsional stiffness. Moreover, usually, built-up members are symmetric, eliminating eccentricities between shear and gravity centers, leading to improved member stability. Built-up cross-sections are built fastening individual profiles with self-drilling screws or alternatively using seam weld (Stone and Laboube, 2005; Li *et al.*, 2014; Wilson and Guzmán, 2011). Research has been focused mainly on open sections such as plain and lipped channels, with simple and complex edge stiffeners, with and without holes and angles (Young and Rasmussen, 1998a; Young and Rasmussen, 1998b; Kesti and Davies, 1999); however, in the past few years, some research on the behaviour of built-up CFS members has been conducted (Georgieva *et al.*, 2012; Yuanqui *et al.*, 2014; Young and Chen, 2008). Currently, the effective width method (EWM) is used worldwide, and the direct strength method (DSM) (Schafer, 2008) is used in North America, for design of CFS structural elements.

Design guidelines in EN 1993-1-3 (2004) for built-up members are still vague. For instance, the EN 1993-1-3 (2004) only predicts that the buckling resistance of closed built-up members should be determined using the buckling curve b in association with the basic yield strength f_{yb} and buckling curve c in association with the average yield strength f_{ya} if $A_{eff} = A_g$.

In fire situation, the design methods presented in the EN 1993-1-2 (2005) for hot-rolled steel members are also applicable to CFS members with Class 4 cross-sections, establishing the same reduction factors for the mechanical properties of hot-rolled and CFSs. Some studies show that the reduction factors for CFS (Outinen, 1999; Kankanamge and Mahendran, 2011; Ranawaka and Mahendran, 2009a) are different from those prescribed in EN 1993-1-2 (2005). Also, the EN 1993-1-2 (2005) for Class 4 cross-sections limits the critical temperature to 350°C, which may be overly conservative if the load ratio is not considered (Ranawaka and Mahendran, 2009b; Heva, 2009). Moreover, there are no specific design guidelines regarding the influence of restrained thermal elongation in the overall behavior of CFS columns in fire. Several studies on this matter were already conducted but for heavy hot-rolled steel columns (Franssen, 2000; Ali and O'Connor, 2001). The great majority of the conducted research on the fire behaviour of CFS columns has been focused on the local and distortional buckling phenomena using both experimental and numerical analysis (Feng *et al.*, 2003a, 2003b; Lee, 2004; Ranawaka and Mahendran, 2006). However, regarding built-

up CFS columns in fire, considering the influence of restrained thermal elongation, research is still very scarce.

In this paper, the most relevant results on the behavior of CFS columns at both ambient and simulated fire conditions are presented (Craveiro *et al.*, 2014; Craveiro *et al.*, 2016). Based on the experimental results, finite element models were developed to accurately reproduce the behavior of CFS columns at both ambient and fire conditions with restrained thermal elongation. This numerical models are fundamental to further investigate the behaviour of CFS columns at both ambient and fire conditions with restrained thermal elongation. Extensive parametric studies will be conducted using the validated finite element models to assess the influence of several parameters, outside the bounds of the experimental tests, such as geometry, slenderness, load levels and restraint levels.

2. Experimental tests
The designed and built experimental test set-ups, for both buckling tests at ambient temperature and fire resistance tests with restrained thermal elongation, are briefly described in this chapter.

In this experimental campaign, four different cross-section shapes were tested, at both ambient temperature and simulated fire conditions with restrained thermal elongation, namely, single lipped channel (C) (Fig. 1 a), open built-up comprising two lipped channels fastened back-to-back on the web (I) (Fig.1 b) and two closed built-up cross-sections comprising lipped channels and plain channels (R and 2R) (Fig. 1 c and d) fastened using self-drilling screws. The cross-section dimensions are also presented in Figure 1 and the total length (L) of the columns was 2.95 m. For the buckling tests at ambient temperature, the cross-sections were instrumented with strain gauges at mid-height of the column, and for the fire resistance tests, type K thermocouples were used. Five sections along the length of the column were instrumented with type K thermocouples.

For the buckling tests at ambient temperature, the experimental test set-up comprised a two-dimensional (2D) reaction steel frame (1), a concrete footing (2), the designed end-support devices (3), a load cell used to measure the applied loading (4), the hydraulic jack (5) used to apply the load to the CFS column and a data acquisition system [Figure 2(a)]. The concrete footing was specifically designed and fabricated for this experimental campaign. To the concrete footing, two steel plates were fixed. The hydraulic jack was connected to the top steel plate of the concrete footing. To the piston of the hydraulic jack, a new set of steel plates were fixed, and to those, the end-support devices were connected. Additional steel plates were placed around the loading system to prevent rotations during loading. In these tests, both pinned and fixed end support conditions were tested, to assess lower and upper
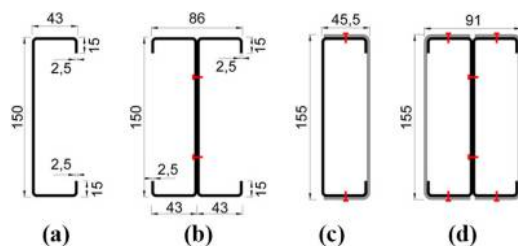
Notes: (a) C; (b) I; (c) R; (d) 2R

Figure 1.
Tested cross-sections

Figure 2.
Schematic view of the experimental test set-ups
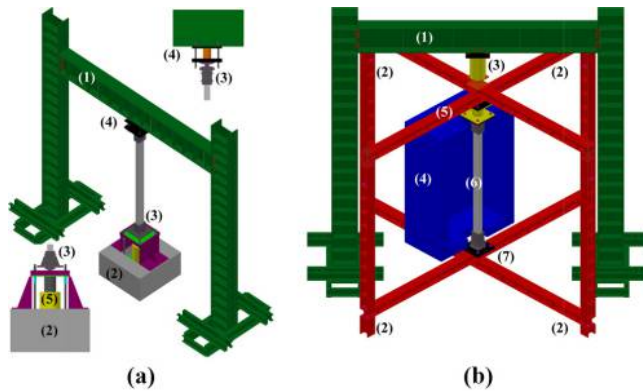
Notes: (a) Buckling tests at ambient temperature; (b) fire resistance tests with restrained thermal elongation

bounds of the buckling load of the tested columns. The loading was applied under displacement control. In all, 24 tests were conducted.

For the fire resistance tests with restrained thermal elongation [Figure 2(b)], the test set-up comprised a 2D reaction steel frame (1) and a three-dimensional (3D) restraining steel frame consisting of four columns, two top and two bottom beams (2) placed orthogonally, used to simulate the stiffness of a surrounding structure to the CFS column subjected to fire. In the fire resistance tests, two restraining frames were used to study the influence of different values of stiffness of the surrounding structure to the CFS column (axial stiffness of 3 and 13 kN/mm). The compressive load was applied using the hydraulic jack (3). The constant compressive load corresponded to the serviceability load (30 and 50 per cent of the design buckling load, $N_{b, Rd}$) applied to the CFS column using the hydraulic jack (3) fixed to the reaction frame (1), and with the nuts of the threaded rods loosened (free body vertical movement of the top beams of the restraining frame), guaranteeing that the compressive load was totally transferred to the CFS column.

The applied service load was controlled by a load cell placed between the top beams of the restraining frame and the hydraulic jack. Reaching the serviceability load defined, the nuts of the threaded rods were tightened (vertical rigid body movement of the top beams was blocked) and from that moment the restraining frame started to exert axial and rotational restraint to the CFS column being tested in fire (6). To measure the restraining forces generated in the testing column during the heating process, a special device was built [(5) in Figure 2(b)], consisting of a hollow steel cylinder where a stiff steel cylinder Teflon (PTFE) lined slides through it. On the top of the stiff steel cylinder, a 500 kN load cell was placed and compressed against the top end plate of the hollow steel cylinder. In these tests, temperature evolution in different points of the cross-section and along the length of the column were monitored, as well as loads and axial and lateral displacements. In all, 96 tests were conducted. Four different cross-section shapes (C, I, R and 2R), two end support conditions (pinned and semi-rigid) and two levels of restraint to thermal elongation (3 and 13 kN/mm; K1 and K2 for pinned conditions, K3 and K4 for semi-rigid conditions) provided by the surrounding structure were tested. For each one of the defined test conditions, three repetitions were performed.

In the buckling tests at ambient temperature axial loads, axial and lateral displacements and strains in the cross-section at mid-length of the column were measured. In the fire resistance tests, serviceability loads, axial forces because of restraint to thermal elongation, temperatures, axial and lateral displacements were measured.

3. Numerical tests

Based on the observed behavior and obtained results, finite element models were developed to accurately reproduce the behavior of CFS columns at both ambient temperature and simulated fire conditions with restrained thermal elongation. In this chapter, a brief description of the finite element models, developed using the commercial software package Abaqus (Simulia, 2010), is presented.

Shell elements are commonly used to model thin-walled structural elements. The S4R element was used to model the steel profiles. Regarding the self-drilling screws, the finite element chosen was the C3D8R.

The material modelling was based on the mechanical and thermal properties of the S280GD + Z steel determined on the experimental tests conducted in the scope of this research. Yield strength, elastic modulus and stress–strain curves that were determined at both ambient and elevated temperatures up to 800°C. The stress – strain relationship of the S280GD + Z steel was modelled considering the methodology presented by Ramberg and Osgood (1943), which was primarily developed to describe stress – strain curves at ambient temperature. The expression based on the Ramberg – Osgood model (Equation (1)) used in this investigation was as follows (Faggiano et al., 2004 and DOT/FAA/AR-MMPDS-01, 2003):

$$\varepsilon_\theta = \frac{f}{E_\theta} + 0.002 \times \left(\frac{f}{f_{y.\theta}}\right)^{n_\theta} \tag{1}$$

The Ramberg–Osgood coefficient was determined based on the provisions presented in DOT/FAA/AR-MMPDS-01 (2003) (Equations 2 and 3):

$$\varepsilon_{us.\theta} = 100\left(\varepsilon_{r.\theta} - \frac{f_{u.\theta}}{E_\theta}\right) \tag{2}$$

$$n_\theta = \frac{ln\left(\frac{\varepsilon_{us.\theta}}{0.2}\right)}{ln\left(\frac{f_{u.\theta}}{f_{y.\theta}}\right)} \tag{3}$$

where ε_θ is the strain at temperature θ (°C), $\varepsilon_{r.\theta}$ is the strain at rupture, $\varepsilon_{us.\theta}$ is the plastic strain at maximum tension load, f is the stress, E_θ is the modulus of elasticity, $f_{u.\theta}$ is the ultimate strength and $f_{y.\theta}$ is the yield strength at temperature θ (°C). The evolution of the parameter n_θ with temperature is presented in Table I for each temperature level.

	Temperature [°C]								
	20	100	200	300	400	500	600	700	800
n_θ	14.602	13.724	8.586	8.353	10.411	13.397	47.024	16.113	11.701

Table I.
N_θ parameter determined for each temperature level

Finally, the stress–strain curves used as input were converted to true stress and logarithmic plastic strain. In Figure 3, the stress and logarithmic plastic strain curves used as input in the finite element model is presented, as well as the relative thermal elongation determined in experimental tests conducted in the scope of this research [20] (Equation (4)). Thermal properties were also determined experimentally using the Transient Plane Source Technique (Craveiro *et al.*, 2016). Residual stresses were not included in the developed finite element models as some investigations previously undertaken have shown that the influence on the ultimate load was less than 1per cent (Ranawaka and Mahendran, 2010):

$$\frac{\Delta l}{l} = 1.10235 \times 10^{-8} \times \theta^2 + 0.68575 \times 10^{-5} \times \theta - 0.79712 \times 10^{-4} \quad 20°C \leq \theta \leq 740°C$$

$$\frac{\Delta l}{l} = 1.1031 \times 10^{-2} \qquad\qquad\qquad\qquad\qquad\qquad 740°C < \theta \leq 890°C \qquad (4)$$

$$\frac{\Delta l}{l} = 2.16443 \times 10^{-5} \times \theta - 8.04389 \times 10^{-3} \quad 890°C < \theta \leq 1000°C$$

The accuracy of the finite element model is governed by the mesh size. Hence, a sufficiently fine mesh shall be used. However, computational resources are limited and it is often necessary to assess the adequate mesh size to obtain accurate results with adequate computational times. A mesh size of 5×5 mm was adopted.

To reproduce accurately the behaviour of CFS columns observed in the experimental tests appropriate boundary, loading and contact conditions, for single and built-up cross-sections, must be defined in the finite element model. Using the capabilities of Abaqus software, hinges, acting as rotational springs, were considered in the boundary condition of the finite element model. The surrounding structure used in the experimental tests was replaced by linear springs (3 and 13 kN/mm) connected to the centroid of the column to be simulated (Figure 4).

Contact between the CFS profiles and between the profiles and the self-drilling screws was modelled assuming a tangential friction coefficient of 0.2 for the contact behaviour in the tangential direction and a hard contact for the contact behaviour in normal direction between the profile surfaces. The surface-to-surface contact was used considering the finite-sliding tracking method to model the interaction between the surfaces of the individual profiles. For the contact between CFS profiles and self-drilling screws, a rough and hard contact was also used.

To simulate ambient temperature tests, displacement loading control was used in the numerical simulations. For the fire tests, load control was used to apply the serviceability load defined for each column. The monitored temperatures in the cross-section and along the

Figure 3.
(a) Logarithmic plastic strain curves for the S280GD + Z steel; (b) relative thermal elongation
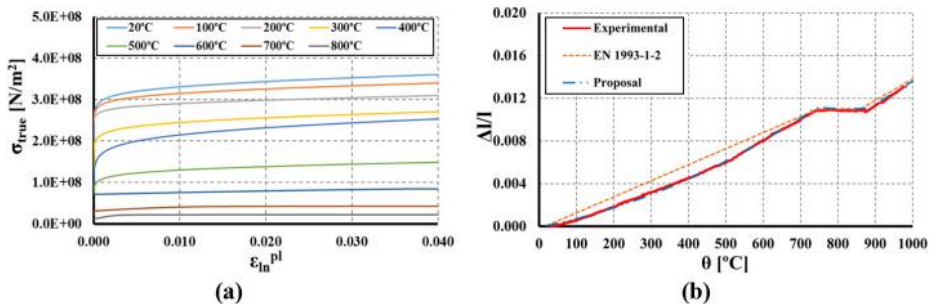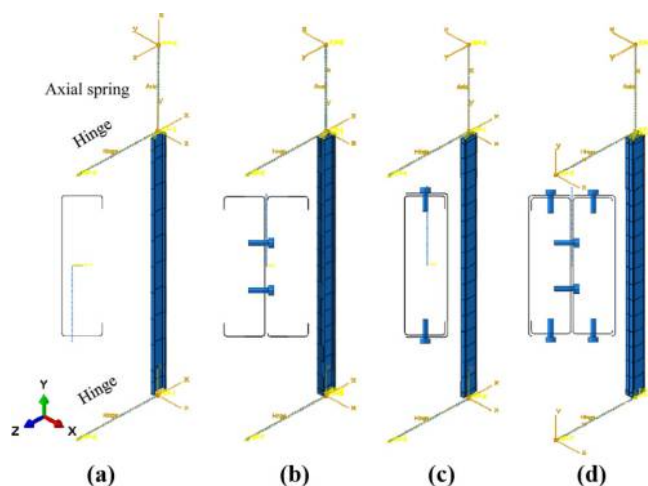
Notes: (a) Lipped channel column; (b) open built-up I column;
(c) closed built-up R column; (d) closed built-up 2R column

Figure 4.
Finite element model
for fire resistance test
with restrained
thermal elongation

length of the column were used as input in the validation process of the finite element model. Influence areas were defined for each thermocouple and its temperature evolution, as a function of time, was allocated to the defined influence area.
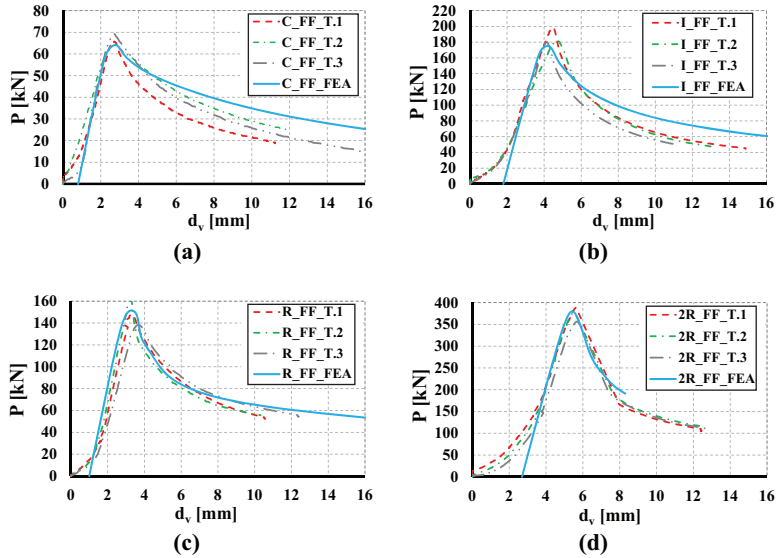
Two different types of analysis were conducted by using the developed finite element model, namely, elastic buckling analysis, to determine critical buckling loads and the associated buckling modes and then a nonlinear static analysis. The buckling modes are then used to input the geometric imperfections in the non-linear analysis. The adopted maximum value for global imperfections was *L/1000*, for distortional imperfections a value of *t* and, finally, for local imperfections *h/200*. Finally, a structural analysis was undertaken to simulate the behaviour of CFS columns. In all structural simulations, the non-linear geometric parameter (*NLGEOM = ON) was active to deal with the geometric non-linear analysis. The developed and calibrated finite element models will be used for future extensive parametric studies to investigate the influence of some parameters, outside the bounds of the experimental tests, on the overall behaviour of CFS columns in fire.

4. Experimental and numerical results
4.1 Buckling tests at ambient temperature
Regarding the buckling tests at ambient temperature, it was observed that the use of built-up cross-sections will ensure significantly higher values of buckling loads. As an example, the obtained results for fixed columns are presented and compared with the numerical results (j_FF_FEA), based on the developed finite element model. A good agreement was observed between experimental and numerical results, both in terms of the buckling loads and axial displacements. These results are depicted in Figure 5. For all tested conditions, a small translation in the axial shortening axis was assumed, for the obtained results of the finite element analysis, as the initial part of the experimental curves was not linear, because of adjustments in the end support devices during the initial loading stage.

Figure 5.
Comparison of the FEA and experimental axial load vs axial shortening curves for all tested cross-sections and fixed-ended supports

Notes: (a) C; (b) I; (c) R; (d) 2R cross-sections

For instance, for fixed-end support conditions, the buckling load of columns with 2R cross-section was 5.6 times higher than the buckling load of columns with lipped channels, 2.01 times higher than the buckling load of columns with open built-up I cross-section and 2.51 times higher than the buckling load of columns with closed built-up R cross-section. Comparing the buckling loads obtained in the experimental tests with the design predictions, based on the EN 1993-1-3 (2004), it was found that the design predictions were conservative for columns with a single lipped channel profile and generally unsafe for columns with built-up cross-sections (two or more profiles). Increasing the number of profiles led to unsafe predictions. The unsafe design predictions for built-up members may be because of the inadequacy of the EWM to deal with built-up members. Also, the spacing of fasteners can influence the failure load. Additional experimental and numerical studies are needed and will be undertaken to further investigate this topic. In Table II, the mean values of the buckling load, obtained in the experimental tests, are compared with the design predictions, based on the EN 1993-1-3 (2004).

Table II.
Comparison between mean experimental buckling loads and design predictions according to EN 1993-1-3

Test	$\overline{P}_{max}$ [kN]	$N_{b.Rd}$ [kN]	Test	$\overline{P}_{max}$ [kN]	$N_{b.Rd}$ [kN]	Test	$\overline{P}_{max}$ [kN]	$N_{b.Rd}$ [kN]	Test	$\overline{P}_{max}$ [kN]	$N_{b.Rd}$ [kN]
C_PP	26.9	24.8	I_PP	75.6	85.51	R_PP	70.0	76.55	2R_PP	253.88	379.07
C_FF	66.4	41.8	I_FF	187.0	187.7	R_FF	149.0	151.1	2R_FF	374.38	443.42

4.2 Fire resistance tests with restrained thermal elongation
The evolution of restraining forces is presented as a non-dimensional P/P_O ratio in function of the mean temperature of the column $(\overline{\theta}_c)$. The mean temperature of the column, $(\overline{\theta}_c)$, is determined using the mean temperature in each one of the five sections, $(\overline{\theta}_{s.i})$, along the length of the column instrumented with type K thermocouples. In these graphs (Figure 7), it is possible to observe the expected behaviour of a column in a real structure. Because of the thermal action and as the column was axially restrained the restraining forces on the column started to increase, while the mechanical properties of the steel degraded with the temperature increase. After reaching a maximum (P_{max}), the restraining forces (P) started to decrease reaching once again the initial service load applied (P_0) to the CFS column. This point defines the critical temperature (θ_{cr}) as the failure criteria in these experimental tests.

In Figure 6, some test results are presented, specifically for the closed built-up R cross-section. The presented results are representative of the remaining tested conditions. Observing the obtained results, the influence of the initial applied load is clear. Increasing the serviceability load from 30 to 50per cent $N_{b, Rd}$, the critical temperatures and critical times decreased for all tested cross-sections.

Concerning the imposed levels of restraint to thermal elongation to the CFS column, it was found that increasing them led to a decreasing on the critical times and temperatures. It was clearly observed, for all tested conditions, that increasing the level of axial restraint to thermal elongation from 3 to 13 kN/mm, the generated restraining forces increase significantly and that the maximum axial load was reached for lower mean temperatures. Also, it was observed that the magnitude of the generated restraining forces was higher for the lower initial load level. For instance, the average magnitude of the generated restraining
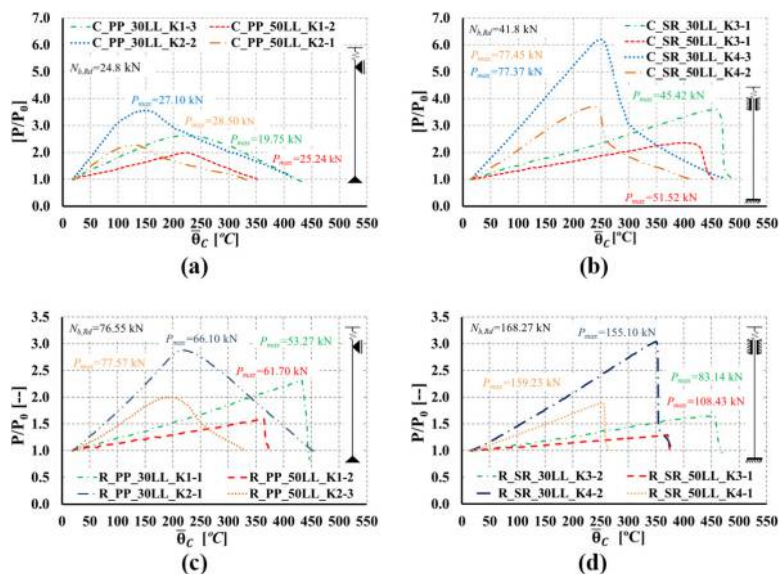
Notes: (a) Pinned C columns; (b) fixed C columns; (c) pinned R columns;
(d) fixed R columns

Figure 6.
Non-dimensional
restraining forces
ratio for lipped and
closed built-up C and
R columns

forces (P-P_0) obtained for the R_SR_30LL_K3 tests was about 32.78 kN whereas for the R_SR_50LL_K3 tests was 25.33 kN.

All experimental results for fixed columns are presented in Figure 7. The critical temperature monitored for all tests is presented as a function of the ratio ($\alpha_k = K_{a,s}/K_{a,c}$ – non-dimensional axial restraint ratio) between the axial stiffness of the surrounding structure to the CFS column ($K_{a,s}$) and the axial stiffness of the CFS column ($K_{a,c}$). For isolated columns under fire conditions subjected to a low level of restraint to thermal elongation, its failure is clearly controlled by temperature increase and by consequent degradation of mechanical properties of the S280GD + Z steel. However, if an isolated column under fire conditions is subjected to a high or very high level of restraint to thermal elongation, then its failure may be controlled by the severity of the generated restraining forces during the heating phase. Consequently, buckling loads may be reached for lower temperatures. Moreover, assuming that the highest critical temperature occurs if the column can freely expand, then it seems that critical temperature reduction is more significant for lower values of the ratio α_k. For higher values of α_k ratio, the temperature decrease becomes smaller.

Lateral deformations were monitored in all experimental tests. In Figure 8, lateral deformation about the minor axis is presented for lipped channel columns, for both pinned

Figure 7.
Variation of critical temperature (θ_{cr}) as a function of the non-dimensional restraint ratio (α_k) for columns with semi-rigid end-support conditions
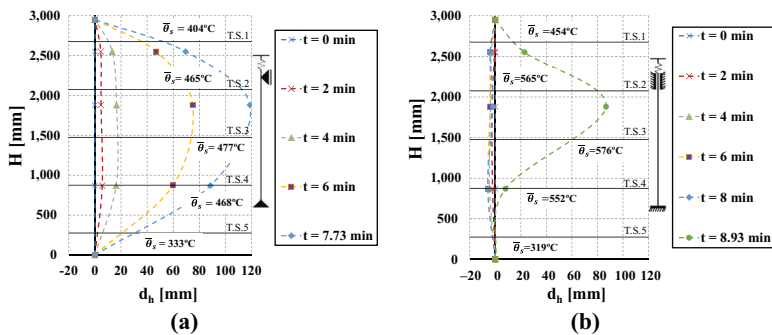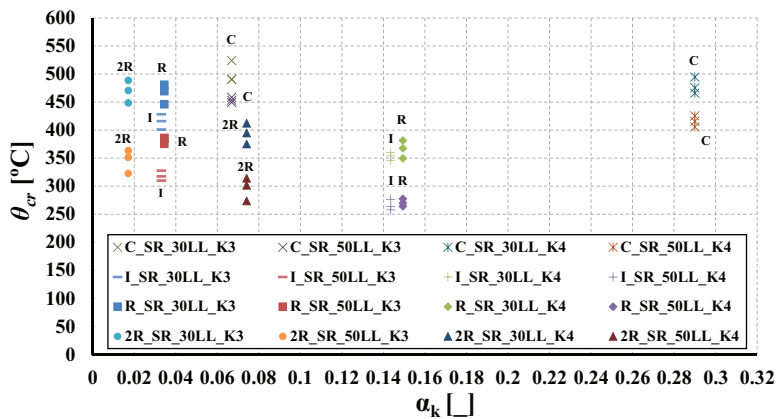
Figure 8.
Lateral deformations about the minor axis for lipped channel columns

Notes: (a) C_PP_30LL_K1-3; (b) C_SR_30LL_K3-1

and fixed end support conditions. The presented results are representative of all test conditions and cross-sections. Lateral deformations about the major axis were also monitored but were found to be negligible.

The validation of the finite element models consisted of comparing the evolution of the non-dimensional ratio between the generated restraining forces during the fire resistance tests with the initial service load (P/P_0) as a function of the mean temperature of the CFS column. It was found that the numerical model can accurately reproduce the behavior of CFS columns in fire with restrained thermal elongation, provided that the mechanical and thermal properties determined in the scope of this investigation at both ambient and elevated temperatures are used as input. In Figure 9, some results for columns with closed built-up R cross-section are presented. The finite element model is in very good agreement with the obtained experimental results. Based on the presented analysis, it is clear that the developed finite element model is suitable to be used in extensive parametric studies outside the bounds of the experimental tests.
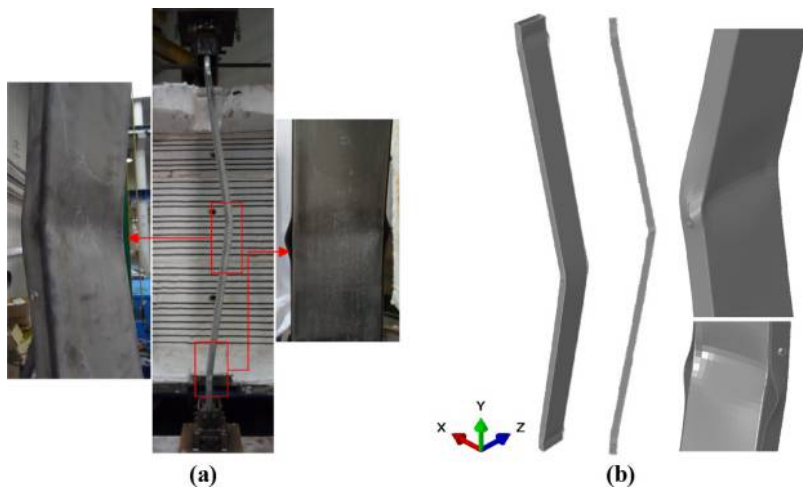
4.3 Failure modes

Generally, for pinned columns, the predominant failure mode was the global flexural buckling about the minor axis. Distortional and local buckling were also observed; however, those buckling modes only become noticeable for large lateral deformations at mid-height of the columns. For semi-rigid support conditions, the predominant failure mode was an interaction between global flexural about the minor axis, distortional and local buckling. Local buckling played a more relevant role on columns with closed built-up cross-sections. In Figures 10 and 11, the final deformed shapes are depicted for semi-rigid columns with C and R cross-sections tested under simulated fire conditions. Also, a comparison between the numerical and experimental final deformed shape is presented. A good agreement was observed between experimental and numerical deformed shapes.
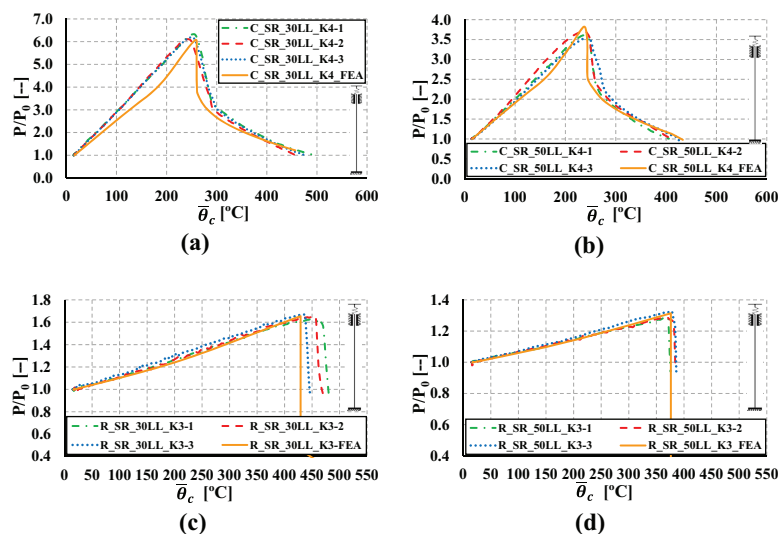
Figure 9.
Comparison between experimental and FEA results for semi-rigid columns with closed built-up R cross-section
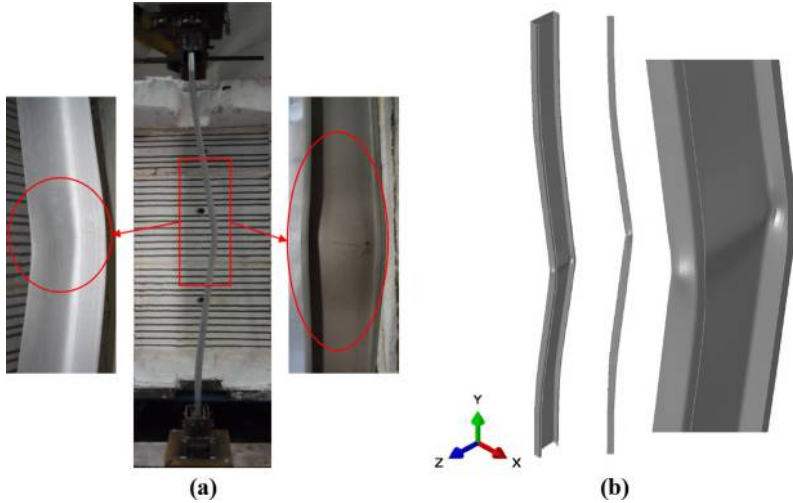
Figure 10.
Experimental (a) and FEA (b) failure modes for semi-rigid lipped channel columns

Figure 11.
Experimental (a) and FEA (b) failure modes for semi-rigid columns with closed built-up R cross-section

5. Conclusions

In this paper, a large experimental campaign on CFS columns at both ambient temperature and simulated fire conditions with restrained thermal elongation is reported. The developed finite element model is also described and the final results regarding the calibration process are presented.

In the buckling tests at ambient temperature, the advantage of using built-up members was clear since the increase in the buckling load was significant. In terms of the design predictions according to EN 1993-1-3 (2004), it was observed that increasing the number of profiles the design predictions become unsafe.

In the fire resistance tests, it was found that the interaction between the initial applied load and the imposed level of restraint to thermal elongation significantly influence the behavior of isolated CFS columns under fire conditions. When some level of restraint exists, additional forces are generated, which may lead to premature collapse and consequently to lower critical temperatures. It seems that increasing the level of thermal restraint the failure of the columns may be controlled by the generated axial restraining forces, whereas for lower levels of thermal restraint, the failure is controlled by temperature increase and consequent degradation of the mechanical properties of the S280GD + Z steel. It seems that the higher reductions on critical temperature, because of restraint, occur for lower values of α_k.

The developed finite element models are able to accurately reproduce the behaviour of CFS columns at both ambient and fire conditions with restrained thermal elongation provided that the mechanical and thermal properties determined in the scope of this research are used as input. Based on the developed and calibrated finite element models, parametric studies shall be undertaken to propose new/improved design methodologies for CFS columns at both ambient temperature and simulated fire conditions, taking into consideration the influence of restrained thermal elongation.

References

Ali, F. and O'Connor, D. (2001), "Structural performance of rotationally restrained steel columns in fire", *Fire Safety Journal*, Vol. 36 No. 7, pp. 679-691.

Craveiro, H.D., Rodrigues, J.P.C. and Laím, L. (2014), "Cold-formed steel columns made with open cross-sections subjected to fire", *Thin-Walled Structures*, Vol. 85, pp. 1-14.

Craveiro, H.D., Rodrigues, J.P.C. and Laím, L. (2016), "Experimental analysis of built-up closed cold-formed steel columns with restrained thermal elongation under fire conditions", *Thin-Walled Structures*, Vol. 107, pp. 564-579.

Craveiro, H.D., Rodrigues, J.P.C., Santiago, A. and Laím, L. (2016), "Review of the high temperature mechanical and thermal properties of the steels used in cold-formed steel structures – the case of the S280GD + Z steel", *Thin-Walled Structures*, Vol. 98 part A,, pp. 154-168.

DOT/FAA/AR-MMPDS-01 (2003), *Metallic Materials Properties Development and Standardization (MMPDS)*, US Department of Transportation, Federal Aviation Administration, Washington, DC, p.1728.

EN 1993-1.2 (2005), *Eurocode 3: Design of Steel Structures. Part 1.2 – General Rules. Structural Fire Design*, European Committee for Standardization, Brussels.

EN 1993-1-3 (2004), *Eurocode 3: Design of Steel Structures, Part 1.3 – General Rules, Supplementary Rules for Cold-Formed Members and Sheeting*, European Committee for Standardization, Brussels.

Faggiano, B., Matteis, G.D., Landolfo, R. and Mazzolani, F.M. (2004), "Behaviour of aluminium alloy structures under fire", *Journal of Civil Engineering and Management*, Vol. 10 No. 3, pp. 183-190.

Feng, M., Wang, Y.C. and Davies, J.M. (2003a), "Structural behaviour of cold-formed thin-walled short steel channel columns at elevated temperatures, part 1: experiments", *Thin-Walled Structures*, Vol. 41 No. 6, pp. 543-570.

Feng, M., Wang, Y.C. and Davies, J.M. (2003b), "Structural behaviour of cold-formed thin-walled short steel channel columns at elevated temperatures. part 2: design calculations and numerical analysis", *Thin-Walled Structures*, Vol. 41 No. 6, pp. 571-594.

Franssen, J.M. (2000), "Failure temperature of a system comprising a restrained column submitted to fire", *Fire Safety Journal*, Vol. 34 No. 2, pp. 19-207.

Georgieva, I., Schueremans, L., Vandewalle, L. and Pyl, L. (2012), "Design of built-up cold formed steel columns according to the direct strength method", *Procedia Engineering*, Vol. 40, pp. 119-124.

Heva, D.Y.M.B. (2009), "Behaviour and design of cold-formed steel compression members at elevated temperatures", PhD thesis, Queensland University of Technology, Brisbane.

Kankanamge, N.D. and Mahendran, M. (2011), "Mechanical properties of cold-formed steels at elevated temperatures", *Thin-Walled Structures*, Vol. 49 No. 1, pp. 26-44.

Kesti, J. and Davies, J.M. (1999), "Local and distortional buckling of thin-walled short columns", *Thin-Walled Structures*, Vol. 34 No. 2, pp. 115-134.

Lee, J. (2004), "Local buckling behaviour and design of cold-formed steel compression members at elevated temperatures", PhD thesis, Queensland University of Technology, Brisbane.

Li, Y., Li, Y., Wang, S. and Shen, Z. (2014), "Ultimate load-carrying capacity of cold-formed thin-walled columns with built-up box and I section under axial compression", *Thin-Walled Structures*, Vol. 79, pp. 202-217.

Outinen, J. (1999), "Mechanical properties of structural steels at elevated temperatures", Licentiate thesis, Helsinki University of Technology.

Ramberg, W. and Osgood, W.R. (1943), "Description of stress-strain curves by three parameters", Technical Note 902, National Advisory Committee for Aeronautics, Washington, DC, p. 27.

Ranawaka, T. and Mahendran, M. (2006), "Finite element analysis of cold-formed steel columns subject to distortional buckling under simulated fire conditions". *Proceeding of the international colloquium on stability and ductility of steel structures*, pp. 747-754.

Ranawaka, T. and Mahendran, M. (2009a), "Experimental study of the mechanical properties of light cold-formed steels at elevated temperatures", *Fire Safety Journal*, Vol. 44 No. 2, pp. 219-229.

Ranawaka, T. and Mahendran, M. (2009b), "Distortional buckling tests of cold-formed steel compression members at elevated temperatures", *Journal of Constructional Steel Research*, Vol. 65 No. 2, pp. 249-259.

Ranawaka, T. and Mahendran, M. (2010), "Numerical modelling of light gauge cold-formed steel compression members subjected to distortional buckling at elevated temperatures", *Thin-Walled Structures*, Vol. 48 Nos 4/5, pp. 334-344.

Schafer, B.W. (2008), "Review: the direct strength method of cold-formed steel member design", *Journal of Constructional Steel Research*, Vol. 64 Nos 7/8, pp. 766-778.

Simulia (2010), ABAQUS/CAE. v. 6.10-1.

Stone, T.A. and Laboube, R.A. (2005), "Behavior of cold formed steel built-up I sections", *Thin-Walled Structures*, Vol. 43 No. 12, pp. 1805-1817.

Wilson, R. and Guzmán, A. (2011), "Evaluation of the slenderness ratio in built-up cold-formed box sections", *Journal of Constructional Steel Research*, Vol. 67, pp. 929-935.

Young, B. and Chen, J. (2008), "Design of cold-formed steel built-up closed sections with intermediate stiffeners", *Journal of Structural Engineering*, Vol. 134 No. 5, pp. 727-737.

Young, B. and Rasmussen, J.R. (1998a), "Tests of fixed-ended plain channel columns", *Journal of Structural Engineering*, Vol. 124 No. 2, pp. 131-139.

Young, B. and Rasmussen, J.R. (1998b), "Design of lipped channel columns", *Journal of Structural Engineering*, Vol. 124 No. 2, pp. 140-148.

Yuanqui, L., Yinglei, L., Wang, S. and Shen, Z. (2014), "Ultimate load-carrying capacity of cold-formed thin-walled columns with built-up box and I section under axial compression", *Tin-Walled Structures*, Vol. 79, pp. 202-217.

Corresponding author

João Paulo Correia Rodrigues can be contacted at: jpaulocr@dec.uc.pt